Modelling the formation of washboards on unpaved highways: a discrete approach.

Spyridoula C. S., Cristian E. B., Andreas R., Daniel S. R.

Master's degree in Modelling for Science and Engineering
Mathematical Modelling Workshop, 2017/2018.

Abstract

Several simulations and models have been purposed till the date, ranging from mathematical analysis to experimentation and simulation, everything with the purpose of gaining some insight about the washboard phenomenon, which has been classified as a complex dynamical system with some chaotic component.

In this project we propose a two dimensional, discrete mathematical model which is translated to an iterative algorithm that tries to reproduce the washboards dynamics observed in the experiments by several authors [1, 2]. As an starting point, the basic discrete model purposed by David C. Mays and Boris A. Faybishenko in 2000, [3], is considered. The lack of realism of that basic model has motivated us to propose new improvements and models for the processes that seem to contribute to washboards formation. To model the road-surface interaction, we propose a probabilistic model for the so-called digging and piling process. To model environmental effects such as diffusion due to wind [4] and bump stability due to gravity [5, 6, 7], a road smoothing strategy that model these kinds of phenomena is proposed.

The dependence of the road profile after some vehicle passes on the initial profile, and the dependence of model parameters on the road surface patterns obtained with our model are also studied and analysed. In addition, a methodology to estimate the wavelength of possible periodic or quasi-periodic regions in the obtained patterns of the road's surface is also proposed.

The implementations of the algorithms we propose and the analysis of the results presented in this report are available in our Git Hub repository [8] for future reproducibility.

Universitat Autònoma de Barcelona

CENTRE DE RECERCA MATEMÀTICA

Contents

1 Introduction

It is commonly and universally observed that under the influence of a flow of vehicular traffic, unpaved roads develop a corrugated profile. This phenomenon, known as washboarding or corrugation, is the appearance of periodic ripples on the surface of unpaved roads and is illustrated by the photographies in figures 1.1a and 1.1b.

(a)

(b)

Figure 1.1: (a) Washboard road study, University of Cambridge. (b) Dirt road showing washboard erosion `https://coloradosprings.gov/rustichills`

Similar phenomena are known to occur on different length and time scales on paved roads, railroad rails [9] and to be related to certain failure modes of computer hard disks. All these phenomena have in common a repeated, nonlinear interaction between a moving source acting on a deformable surface [10]. According to several authors washboard patterns are not uniformly all along the length of the road, but contain irregularities [3].

Differently to what expected, the downward forces on the surface coming from the vehicles do not smooth the road. Dirt roads do not heal themselves, but instead become progressively more corrugated [4].

Typically, the corrugations have a wavelength between 0.5 and 1m, and amplitude up to 50mm [4]. Their impact on the vehicles passing over is harmful and uncomfortable, and the usefulness of the roads is severely impaired. Washboarding bedevils transportation worldwide, as this phenomenon is not only disturbing for the drivers, but also poses as a hazard due to the fact that the adherence of the road, and as a result the control of the vehicle is reduced. Furthermore, from an economic point of view, unpaved roads mainly in developing countries hold a great economic significance, as they carry a substantial proportion of the total traffic [1, 2, 11].

An important parameter that influences the appearance and form of the corrugations is the speed of the vehicles, as the washboarding occurs when vehicles drive above a critical speed [11]. Other influential parameters include car mass, the characteristics of the tires and the softness of the ground [1, 4]. The suspension of the vehicle is known not to affect the corrugation, as ripple frequencies are generally quite far from the resonant frequencies of the suspension, and ripples can appear even with no suspension present [10]. In Table 1.1 are summarized these influential and non-influential parameters.

Table 1.1: Possible influential parameters

Influential	Non-influential
Vehicle velocity: 10-25 $\frac{m}{s}$	Vehicle suspension
Vehicle mass	
Tire (pressure, diameter, softness)	
Number of vehicle passes	
Softness/fineness of ground	

Early attempts at explaining the origin of road corrugation proposed that the washboarding was a result of moving wheels that push grains ahead of them as they roll and the grains pile up in front of the wheel. Later experiments by Mather [12] with both driven and idling wheels, showed that this does not occur. He proposed that the origin of the road instability is the bouncing motion of the wheel, caused by random irregularities on the ground. When the wheel passes through the uphill side, is later launched into the air for some brief time and lands again after a distance. This has, as a result, to spray sand away and creating the next pile of the developing corrugation pattern, and afterwards the motion repeats itself. Thus, the result of the washboarding is not the piling of grains itself, but rather the impact of the vehicle on the ground. Mather's picture is similar to other surface instabilities involving granular materials, such as the ripple patterns appeared in windblown and underwater sand [2, 4, 9].

The engineering interest in washboard derives from the importance to understand all the complexities of the system, to predict and to reduce or eliminate the effect [2]. Many engineering models and simulations of washboard formation exist, from damped pendulum models to full continuum simulations of the road surface. The simplest system, which studies the washboarding phenomenon as a nonlinear, pattern forming instability, has also been studied. Furthermore, numerous experimental studies have been done, from laboratory-scale to full-scale road tests [2].

The aim of this project is to produce and present an enhanced model for simulation of washboards in unpaved roads, by creating an iterative algorithm that reproduces the washboard dynamics observed in the experiments of several authors. Instead of solving the system analytically, the road and its components are defined as discrete parts, as proposed by David C. Mays and Boris A. Faybishenko in 2000 [3].

2 Problem approach

In this section we will explain thoroughly the qualitative aspects of our washboarding model.

The main cause behind the washboarding effect in a unpaved road is observed to be the presence of vehicles travelling across it. The tires of these vehicles press the soil and project some particles of it backwards, causing what we call digging and piling effects. Basically, some grains of soil are being displaced from certain positions and added to others, leading to irregularities in the road. This projection of soil particles can be due to the rotation of the wheels (see Figure 2.1a): if the vehicle is moving forward, the friction force between the wheel and the soil points backwards with respect to the soil, so the loose grains in contact with the tire are projected backwards. This phenomenon may happen at any given instant if the soil of the road is extremely loose.

(a)

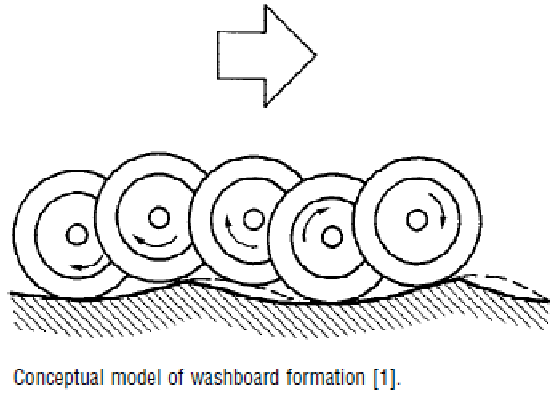

(b)

Figure 2.1: (a) Digging effect by wheel slipping (b) Conceptual model of washboard formation by successive jumping and digging events, [3].

Instead, we will consider more typical (not extremely loose soils) roads so that the digging effect we have explained only happens at certain instants that we concrete now. The typical situation where digging occurs is when a wheel finds a bump in the shape of the road, when passing through it the wheel performs a small jump taking off from the position of the bump, and it finally lands again on the road after advancing some distance. As suggested in [3], when the wheel lands is when the digging event occurs (Figure 2.1b).

Thus, the main engine of this phenomenon according to the model approach we consider, is this jump-dig mechanism. However, there are other aspects that should have to be taken in consideration. With the explained mechanism by itself, the problem is that if we focus on a certain bump, there is a position in front of this bump, separated from the bump by the jump length associated to this bump, where several wheel landings will probably occur in future vehicle passes causing a lot of digging. Consequently, in this region the soil level will continuously decrease while the soil level of the region prior to the landing spot will continuously increase (piling effect).

For this reason, we propose a probabilistic digging procedure to model the fact that "the deeper one tries to dig, the harder or less probable it is". In addition, we have considered to add some other mechanisms to the basic model [7] taking into consideration some reasonable smoothing effects; for example, soil diffusion or the effect of gravity on the bumps stability.

Regarding these smoothing effects, we propose two types of them: deterministic or probabilistic. An example of deterministic smoothing mechanism would be the one we have called slope smoothing. This one takes into consideration the fact that very spiky bumps are unstable so, setting the maximum slope of a bump, prevents their emergence. On the other hand, an example of a probabilistic mechanism would be the wind. This basically takes some random grains of soil and places them randomly elsewhere or at positions with minimal height.

3 Discrete model

In this section we discuss the basic discrete model structure from which we have been able to perform computer simulations. The main algorithm is also presented.

Following the same initial approach as it is done in [3], we model the road soil as a set of $r \geq 1$ columns (piles) labelled by their horizontal position $x_i = i \in \{0, 1, 2, ..., r-1\}$, and assume periodic boundary conditions. In this way, the r-th pile corresponds to the 0-th pile. Thus, in fact we are dealing with a circular roadway.

In our approach, we assume a non-penetrable *ground level* that no vehicle can pass through. Moreover, we define a *standard road height*, h_0, which can be thought as the height that a road would have if no vehicle passes through it. In Figure 3.1 the ground level is represented by a line of `####`, and the standard height is equal to six block units. Since a real road cannot be perfectly flat, we consider that initially, some random irregularities are present, so that at some positions the road's height is higher than the standard road's height. In Figure 3.1 we have considered five soil blocks to represent these irregularities, although more complex and random configurations can be considered.

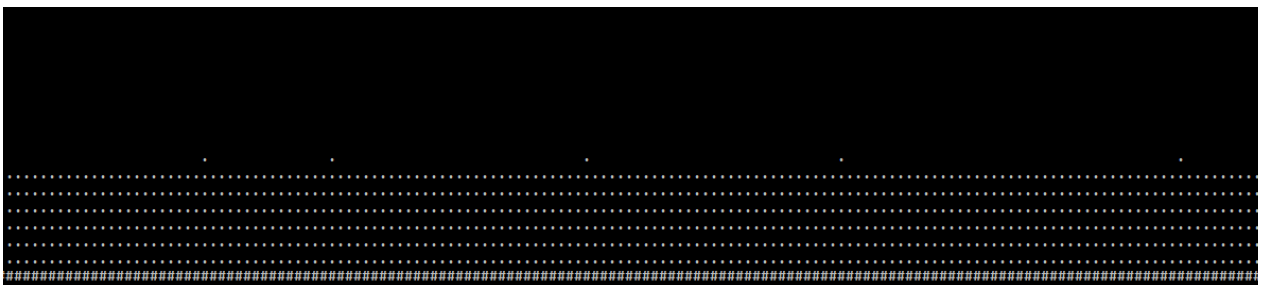

Figure 3.1: Discrete representation of the road with some random irregularities above its standard/initial height equal to 6 block units.

Another important assumption in our model is the fact that we model vehicles as **mono-wheel** vehicles with a certain diameter **d** [1]. Moreover, we use the notation $\texttt{wheel}_{x_f}$ and $\texttt{wheel}_{x_0}$ to refer to the right-most and left-most positions of the wheel, respectively. The wheel is moving from the left to the right in our simulations.

As it was qualitatively described in section 2, our discrete model can be simulated by iterating over wheel passes through the road. We denote by $f_{ij} = f(x_i, j)$ the height of the road at position x_i and iteration j; equivalently, it is the number of block units that form the i-th column of our discrete road at the j-th iteration. If for some explanations the iteration index is not relevant, we will omit it. With this notation we define the elevation of the wheel as the height of the road at the right-most part of the wheel, that is $\texttt{wheel}_e = f(\texttt{wheel}_{x_f})$.

In Algorithm 1 we present pseudo-code for the main procedure that allows to simulate successive wheel passes according to our model. We have followed a Object Oriented approach. The `input arguments` needed to perform the simulation and their descriptions are the following:

- `road`: a Road object having all the intrinsic properties described above.
- `wheel`: a Wheel object having all the intrinsic properties described above.

[1] In fact, this parameter we refer to as **d**, should be interpreted as a digging width which may not coincide with the diameter of the wheel. However, for an easier understanding of the model, we can think of it as the actual diameter of the wheel.

- max_iterations: maximum number of wheel passes (iterations).
- bump_method: method name for determining the height of a given bump.
- dig_method: method name for the digging procedure.
- dig_probability_arguments: probability distribution arguments for the corresponding digging method.
- smoothing_method: method name for the smoothing procedure.
- smoothing_arguments: extra arguments needed depending on the smoothing method chosen.

Algorithm 1 Simulation algorithm

```
procedure simulation( input arguments )
    current_vehicle_passes ← 0                    ▷ Initialise the number of vehicle passes
    while number_of_passes < max_iterations do

        if ( current_vehicle_passes < number_of_passes ) then
            smoothing(road, extra_arguments)      ▷ Smooth the road after a vehicle pass
            current_vehicle_passes ← number_of_passes
        end if
        initial_position ← wheel_{x_f}
        bump_position ← move_to_next_bump(road, vehicle, extra_arguments)
        bump_height ← determine_bump_height(road, vehicle, extra_arguments)
        jumping(road, vehicle, bump_height)                   ▷ Makes the wheel jump
        digging(road, vehicle, digging_arguments)   ▷ The digging and piling events occur

        Update some vehicle (wheel's) features such as the current elevation and the position
    after jumping.     ▷ After jumping, the wheel is moved d units to the right and its elevation is
    updated at the height of position wheel_{x_f}
        final_position ← wheel_{x_f}.

        if ( final_position < initial_position ) then
            number_of_passes += 1                         ▷ A vehicle pass has finished.
        end if
    end while
end procedure
```

Heuristically, the simulation procedure is the following: lets imagine that the $i-1$-th vehicle has passed through the road (i.e. that it has surpassed the r-th position of the road so it starts to appear at the beginning of the road due to periodic boundary conditions). At this time, the i-th iteration of the simulation starts:

1. The first (next) bump is localized and the wheel is moved to the beginning of it.
2. The height of the bump is determined.
3. The wheel jumps some horizontal distance that will depend on the computed bump height.
4. Digging and piling events are performed due to the wheel landing on the road.

5. Repeat 1. to 4. until the end of the road has been reached.
6. The road surface undergoes smoothing effects due to environmental phenomena such as wind, rain, gravity,...
7. Repeat 1. to 6. until `max_iterations` wheel passes have been performed.

3.1 Modelling the vehicle - road surface interaction

3.1.1 Jumping distance

As a rule to compute the distance **L** that a car jumps after encountering a bump of height **h**; we follow the model proposed by [3] which basically assumes that the vehicle follows an ideal parabolic trajectory when jumping, and that the velocity components of the wheel depend linearly on the bump's height. Then, the expression proposed to compute **L** has the following form:

$$\mathbf{L} = \beta \mathbf{h}, \tag{3.1}$$

where $\beta = \frac{\gamma v_x}{km} > 0$ is a proportionality constant that includes dependences on the velocity v_x, the mass m supported by the wheel, the suspension stiffness k and an unknown factor γ that would en globe other possible influential factors and such that β is a dimensionless number.

As an example, in Figure 3.2 we see that if a wheel of diameter **d** finds a bump at position x_1, and assuming that just before jumping the right-most part of the wheel is at position x_0, then after jumping, the right-most part of the wheel will be located at position x_{L+d}. Since $\mathbf{h} = 1$ and $\beta = 15$, one can check that $\mathbf{L} = 15$. As expected, it is the distance between $\texttt{wheel}_{x_f}$ before the jumping and $\texttt{wheel}_{x_0}$ after landing on road.

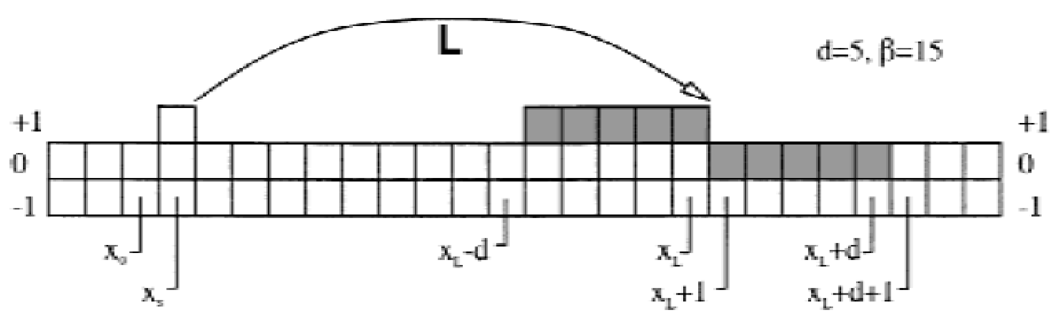

Figure 3.2: Graphical representation of the jumping, and then digging and piling events. [3].

Assuming a fixed value of γ, an increase of the value of β would mean either considering vehicles travelling at higher velocities, or having less massive vehicles, or vehicles with softer wheel suspensions (i.e., more flexible suspensions).

3.1.2 Bump height determination

Imagine that at some point of the simulation the wheel finds a bump which starts at position $x_0 + 1$ (see Figure 3.3). When the wheel arrives just in front of it so that $\texttt{wheel}_{x_f} = x_0$, it will jump a distance **L** which depends on **h** according to formula (3.1). The approach considered to compute this bump height is given by the following expression:

$$\mathbf{h} = \max\{f(\mathbf{x}) \mid \mathbf{x} \in [x_0 + 1, x_0 + \mathbf{d}]\} - f(x_0) \tag{3.2}$$

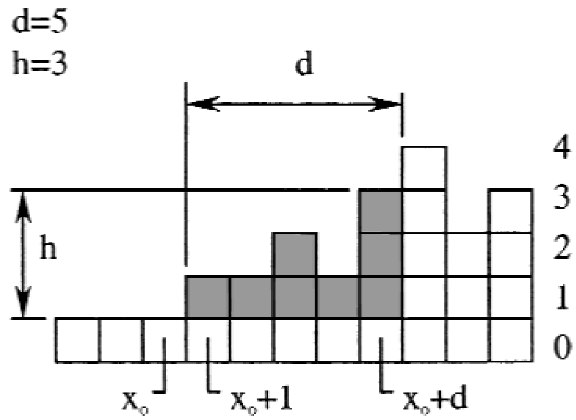

Figure 3.3: Determination of discrete bump height. Picture taken from [3].

In order to explain our justification for the bump-height criteria given by equation (3.3), assume for simplicity that the wheels are cubic with edges of length **d**. Basing our arguments in empirical facts about the separation between bumps and so, we would say that the vehicles' wheels will not be able to do more than a quarter of round without escaping from the bump. Equivalently, the wheel will not be able to climb a bump a distance larger than its diameter.

With this, it is reasonable to expect that bumps achieve its maximum more or less and at most **d** units distance from its starting point.

A generalisation of this approach would be:

$$\mathbf{h} = \max\{f(\mathbf{x}) \mid \mathbf{x} \in [x_0 + 1, x_0 + w]\} - f(x_0) \tag{3.3}$$

where $w \in \mathbb{Z}/(r)$.

Note that since our model is discrete, we must have $\mathbf{L}, \in \mathbb{Z}$ and therefore $\mathbf{h}, \beta \in \mathbb{Z}$. Without loss of generality we also assume that cars always move from left to right so that $\beta \in \mathbb{Z}^+$.

3.1.3 Digging model

The simplest criteria that one could imagine for digging and piling, is that for each position above the wheel that has landed after jumping, a block of soil is removed and put backwards in the associated position, that is:

$$f_{\text{after}}(\mathbf{x}) = \begin{cases} f_{\text{before}}(\mathbf{x}) - 1 & \text{if } x_L < \mathbf{x} \leq (x_L + \mathbf{d}) \\ f_{\text{before}}(\mathbf{x}) + 1 & \text{if } (x_L - \mathbf{d}) < \mathbf{x} \leq x_L \end{cases} \tag{3.4}$$

where we are using the notation from Figure 3.2. This means that the height of the road is modified each time that the wheel jumps and with probability one. This approach is the one considered in [3], and it is seen to lead to washboards with increasing amplitude over iterations.

Since the above case is quite unrealistic, we consider new approaches that try to model the reality and account for the fact that “the deeper one tries to dig, the harder (less probable) it is to dig”.

Algorithm 2 General digging algorithm

```
procedure digging( road, wheel, dig_probability_function, dig_probability_args )
    remove_from ← positions where the digging event may occur
    put_on ← positions where the piling event may occur
    random_probabilities ← generate #(wheel's diameter) random numbers between 0 and 1.
    dig_probabilities ← dig_probability_function(road.piles[remove_from], dig_probability_args)
    increments ← (random_probabilities ≤ dig_probabilities).astype(int)

    road.piles[remove_from] -= increments
    road.piles[put_on] += increments
end procedure
```

Algorithm 2 gives a general digging strategy, which in particular includes the one considered in [3] by choosing as probability distribution function the constant function with value 1 (always dig) as we are going to explain.

Constant probability distribution

This simple approach consists in choosing a constant probability $p \in (0, 1]$ and then, for each position $x \in (x_L, x_L + \mathbf{d}]$, remove a block of soil from that position with probability p and put it into the associated backwards position $x - \mathbf{d}$. Note that mathematically, this is equivalent to use equation (3.4) but adding or subtracting according to the probability p. The case when $p = 1$ is the one considered in [3]. Following the notation from Algorithm 2 we have that `dig_probabilities` $= (p, ..., p)$.

Quadratic probability distribution

Since we want to account for the fact that *“the deeper one tries to dig, the harder (less probable) it is to dig”*, the first approach we considered was to use a quadratic function f_q as probability density function:

$$f_q(h) = Ah^2$$

where h refers to the road’s height at some position and A a normalization constant. Now, since one of our hypothesis was that we cannot dig below the ground level (road’s height $= 0$), and imposing that the probability of digging when the road's height is equal to the *standard road's height* h_0 is one [2], the normalization condition is:

$$1 = \int_0^{h_0} f_q(h)dh = A \int_0^{h_0} h^2 dh \implies A = \frac{3}{h_0^3} \implies f_q(h) = \frac{3h^2}{h_0^3} \tag{3.5}$$

In particular, the probability of digging at some position where the road's height is h will be:

$$P_q(h, h_0) = \frac{h^3}{h_0^3}, \qquad 0 \leq h \leq h_0 \tag{3.6}$$

and we generalize it to

$$P_q(h, h_0) = \begin{cases} 0 & h < 0 \\ \frac{h^3}{h_0^3} & 0 \leq h \leq h_0 \\ 1 & h > h_0 \end{cases} \tag{3.7}$$

Note that this probability distribution that depends on the road's height is uniquely determined when fixing the threshold h_0. This does not allow us to vary any parameter and be more or less strict when deciding about digging or not digging. For this reason we consider a better probability model that allows us to do that.

Tailed-exponential probability distribution

Following the same idea as for the quadratic distribution, we now consider a probability density distribution in a exponential form:

$$f_e(h) = Ae^{\alpha h}$$

We impose the following normalization condition,

$$1 = \int_{-\infty}^{h_0} f_e(h)dh = \frac{A}{\alpha} \int_{-\infty}^{h_0} \alpha e^{\alpha h} dh \implies A = \frac{\alpha}{e^{\alpha h_0}} \implies f_e(h) = \frac{\alpha e^{\alpha h}}{e^{\alpha h_0}} = \alpha e^{\alpha(h - h_0)} \tag{3.8}$$

and as probability distribution function we use,

$$P_e(h, \alpha, h_0) = \begin{cases} 0 & h < 0 \\ e^{\alpha(h-h_0)} & 0 \leq h \leq h_0 \\ 1 & h > h_0 \end{cases} \tag{3.9}$$

Note that now we can vary parameter α which is able to model the stiffness of the soil in some sense as we can see from Figure 3.4. In addition, by letting $\alpha = 0$ we recover the uniform or constant probability with $p = 1$.

[2] We could choose any other threshold value as h_0, but the one it is more realistic for us is to chose h_0 as the standard road's height we defined at the beginning of section 3.

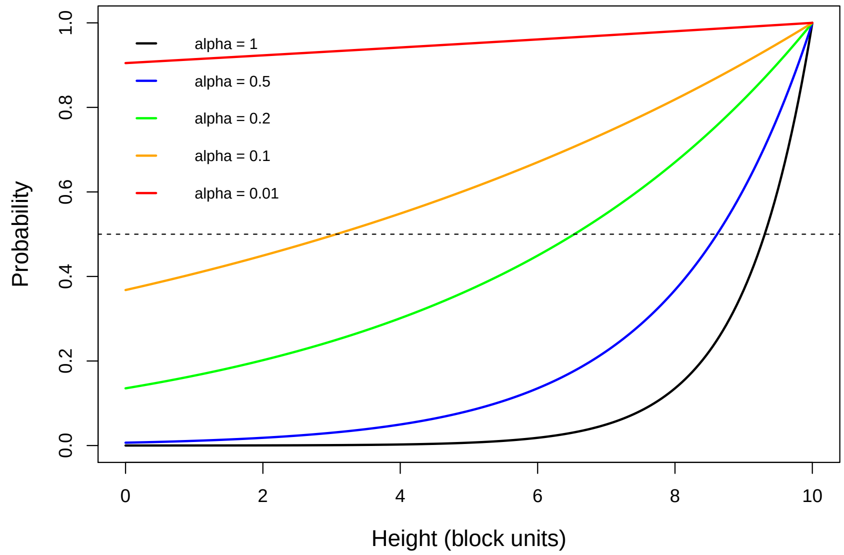

Figure 3.4: Probability distribution function (equation (3.9)) for the tail-exponential case for the values of α in the set $\{0.01, 0.1, 0.2, 0.5, 1\}$ and choosing as normalization height $h_0 = 10$.

The higher the value of α, the harder is to dig for deeper heights, and vice-versa. Thus, a large value of α would model a very stiff road soil, whereas smaller values would model soft materials. In addition, this parameter would also account for tire pressure, something that is not accounted by the constant ($p = 1$) digging model proposed in [3].

3.2 Modelling environmental phenomena: road smoothing

So far we have been considering only the interaction between vehicles and the road. In addition to vehicles, there are other possible factors that would affect and modify the profile of the road during the day although no vehicle passes. Among these factors, we have considered two that may be essential: diffusion and bump stability.

3.2.1 Diffusion

In our context, diffusion effects would refer to events such as some portions of soil being transported from one point of the road to another by diffusion through the air. This transport of soil grains may occur due to the presence of natural wind currents, or even due to wind currents generated by the pass of vehicles travelling at relatively high speeds. For the typical continuous model for washboards formation that is currently seen in the literature (see for example [4]), it is common to include a diffusion term on the differential equations that describe the evolution of the road's surface.

In order to account for diffusion effects during a simulation of our discrete model approach, we have basically built one deterministic and one random functions that simulate the effect of wind moving some blocks or grains of soil from one place of the road to another; these functions are called `wind_smoothing` and `random_wind_smoothing`, respectively.

For our work, we are going to focus on using the random approach, since it is more realistic. The pseudo-code of the random wind approach is given in Algorithm 3.

Algorithm 3 Random wind smoothing algorithm

```
procedure random_wind_smoothing( road, h_max )
    while max_height(road) > h_max do                ▷ max_height(road) = max_{0≤i<r} {f(x_i)}
        for i ∈ {0, 1, ..., r − 1} do
            if f(x_i) > h_max then
                temporal_minimum ← min(road)          ▷ min(road) = min_{0≤i<r} {f(x_i)}
                temporal_min_positions ← {x_i such that f(x_i) = temporal_min}
                chosen_position ← random_choice_from(temporal_min_positions)  ▷ Some x_j

                road.add_soil(x_i)                    ▷ For example, f(x_i) ← f(x_i) + 1
                road.remove_soil(chosen_position)     ▷ f(x_j) ← f(x_j) − 1
            end if
        end for
    end while
end procedure
```

3.2.2 Bump stability

Imagine the situation of having a pile of sand on top of a flat surface. Due to the action of gravity, if we start putting more and more sand onto the pile to try to increment its height as much as possible; at some point the sand on the top would start falling down the sides (avalanches). In fact, this is what is observed in reality, and depending on the properties of the soil, such as the softness, the density or the grain sizes, the maximum stable height that a pile of sand would reach will vary.

With the assumptions we have done so far in our models, in principle we are enabling the bump height $\mathbf{h}$ to be indefinitely large [3]. Thus, the precedent paragraph motivates us to be more restrictive and consider a simple model that accounts for a maximum bump height that the simulated road can achieve. The function that does that is called `max_smoothing`, and given a maximum height h_{max} all the grains above that height are removed and put into lower and neighbour positions.

On the other hand, the implementation of our model without any smoothing procedure, has led to situations where three or more blocks of soil were one on top of the other so that the slope of the road in that position was too large to be realistic (i.e., physically stable). Moreover, in the literature [5, 6, 7], some models have been proposed to determine the shape of sand piles, mainly based on the so called angle of repose θ_r. The idea is that a bump or pile of that soil would acquire a different shape characterized by a different angle of repose depending on the properties of the soil. With these ideas, our proposal is to design a smoothing procedure that avoids the presence of such steep and sharp configurations and profile the bumps of the road according to some angle of repose that partially characterizes the type of soil.

So far we have implemented `slope_smoothing` function which can be applied to the road's profile iteratively to eliminate very steep configurations after some iterations.

[3] Of course depending on the value for the parameter α if we use the tailed-exponential probability distribution, or the value of the constant probability p if we use a constant probability distribution.

Algorithm 4 Slope smoothing algorithm

```
procedure slope_smoothing( road, slope )
    for i ∈ {0, 1, ..., r − 1} do
        j ← (i + 1) mod(r)
        slope_i ← f(x_i) − f(x_j)            ▷ Minus the usual discrete slope at [x_i, x_j]
        if slope_i > slope then
            road.add_soil(x_j)               ▷ f(x_{i+1}) ← f(x_{i+1}) + 1
            road.remove_soil(x_i)            ▷ f(x_i) ← f(x_i) − 1
        else if slope_i < −slope
            road.add_soil(x_i)               ▷ f(x_i) ← f(x_i) + 1
            road.remove_soil(x_j)            ▷ f(x_{i+1}) ← f(x_{i+1}) − 1
        end if
    end for
end procedure
```

However, asymptotically this function is able to make the bumps tend to an angle of repose of

$$\theta_r = \arctan(\texttt{slope}) \cdot \frac{360}{2\pi} \tag{3.10}$$

degrees, for integer values of $\texttt{slope} \geq 1$. Thus, the minimum angle of repose we are able to achieve with this procedure, is when $\texttt{slope} = 1$, which leads to an angle of repose $\theta_r = 45^{\text{o}}$.

A future work would be to implement some algorithm that allows to fix an arbitrary angle of repose θ_r and smooth the road profile accordingly. It is observed in many materials that the angle of repose is usually below or about 45º [13], so the challenge would be to implement a new algorithm that allows us to achieve smaller angles.

3.2.3 Smoothing strategy

We have been experimenting with different smoothing strategies, which consists in combining and alternating the usage of the different smoothing functions that we have commented in the subsections above. However, in order to simplify our work and do not overextend too much, we have chosen a default smoothing strategy [4] which we now explain. As a reference, the pseudo code is shown in Algorithm 5.

This strategy is structured in three main parts:

1) First, we account for the wind or general diffusion effects, present with a certain probability p_w, by applying the `random_wind_smoothing` procedure to move blocks of soil that are located at heights above a threshold $h_{\text{max,wind}}$ to positions where the road's height is minimum. The max() function call that we consider to define $h_{\text{max,wind}}$ is made such that we do not allow the diffusion effects to affect blocks of soil that are below the threshold $h_0 + \Delta h_{0,\text{wind}}$. Then, for the rest of the cases for which $h_{\text{max,wind}} = h_{\text{max}} - \Delta h_{\text{max,wind}}$, we are removing the $\Delta h_{\text{max,wind}} \in \mathbb{Z}^+$ higher levels of the road's surface and putting them (by means of the random wind function) to positions with minimum height.

   The advantage of this procedure is that it dynamically works as the maximum road height is varying along the simulation. The parameter $\Delta h_{\text{max,wind}}$ would be directly proportional to the

[4] In our program it is labelled as `'strategy 3`.

wind's strength or velocity. Similarly, $\Delta h_{0,\text{wind}}$ would be related to how turbulent (vorticity) is the wind (the more turbulent the smaller the value of this parameter).

Algorithm 5 Default smoothing strategy algorithm

procedure **`smoothing_strategy`**(`road`, `args` : $\{h_{\max}, \texttt{slope\_iters}, \Delta h_{\max,\text{wind}}, \Delta h_{0,\text{wind}}, p_w\}$)
 $p_{\text{random}} \leftarrow \texttt{uniform}(0,1)$

 if $p_w > p_{\text{random}}$ **then**
  $f_{\max} \leftarrow \max(\texttt{road})$ ▷ Current maximum height of the road
  $h_{\max,wind} \leftarrow \max\{h_{\max} - \Delta h_{\max,\text{wind}}, h_0 + \Delta h_{0,\text{wind}}\}$
  `random_wind_smoothing`(`road`, $h_{\max,\text{wind}}$) ▷ Smoothing for wind effects
 end if

 `max_smoothing`(`road`, $h_{\max}$) ▷ Smoothing for bump stability (local avalanches)

 for $i \in \{1, ..., \texttt{slope\_iters}\}$ **do**
  `slope_smoothing`(`road, slope = 1`) ▷ Smoothing for bump stability (angle of repose)
 end for

end procedure

2) Then the `max_smoothing` procedure enters in action. For all blocks of soil that are located at a height above $h_{\max}$, they are removed and replaced in neighbour positions (and with lower road heights). This would simulate local avalanches of the bumps of soil, and the value of $h_{\max}$ may depend on the properties of the material.

3) Finally, a number of `slope_iters` iterations of the `slope_smoothing` procedure are performed to profile the road's surface and make it slightly tend to an angle of repose of 45º. As we commented before, it would be good to improve this approach by being able to consider smaller angles of repose.

In the next section we present the parameters of our Python implementation of the model and also some default values we will use for obtaining and analysing results.

3.3 Simulation implementation in Python

In tables A.1, A.3 and A.5 in Appendix A, we summarize the variables that can be varied to run our simulation program. The code is available at the GitHub repository of the project [8].

In Table 3.1 we show the default parameters that will be used for all the simulations discussed in section 4, unless we specify values for some of the variables explicitly.

Table 3.1: Default parameter values. The descriptions can be found in the Tables from Appendix A

Variable	**Notation**	**Default value**
`number_of_wheel_passes`	`max_iterations`	1000
`road_size`	r	500
`standard_height`	h_0 (road's standard height)	100
`nr_of_irregular_points`	——	50
`wheel_size`	**d**	10
`velocity`	β	11
`dig_method`	——	`Backwards tailed exponential`
`h0`	h_0 (normalization height)	h_0 (road's standard height)
`alpha`	α	1
`smoothing_method`	——	`strategy 3`
`h_max`	$h_{\max}$	$h_0 + \Delta$, $\Delta = 3$
`increment_h_max_wind`	$\Delta h_{\max,\text{wind}}$	1
`lower_bound_increment_h_max_wind`	$\Delta h_{0,\text{wind}}$	3
`p_wind`	p_w	0.2
`slope`	`slope`	1

Note that we have used the notation h_0 for two things: one refers to the road's standard height and the other refers to the threshold height used to normalize the dig probability distributions. Since by default we are considering that both h_0 are the same (the road's standard height), there would be no confusion.

3.4 Assessing periodicity of road surface patterns

Inspired by the definitions and notions of autocorrelation function found in [14] and [15], and accounting for the fact that our road, and thus the road's surface profile data, is circular due to periodic boundary conditions (period of length r); we give the following definition for the (discrete) biased Autocorrelation Function (ACF):

$$R_f(k) = \frac{\sum_{i=-k}^{r-1-k} (f(x_i) - \hat{\mu})(f(x_{i+k}) - \hat{\mu})}{\hat{\sigma}^2}, \qquad k \in \{0, 1, ..., r-1\} \tag{3.11}$$

where $\hat{\mu} = \frac{1}{r}\sum_{i=0}^{r-1} f(x_i)$ is the observed mean of road heights and $\hat{\sigma}^2 = \sum_{i=0}^{r-1}(f(x_i) - \hat{\mu})^2$ the observed variance. This definition can be used for any discrete function f taking values at some points $x_0, x_1, ..., x_{r-1}$. Usually the $R_f(k)$ we have defined in equation (3.11) is divided either by $n-k$ or n, depending on if it is preferred an unbiased or a biased estimator of the usual autocorrelation function, respectively. However, we prefer not to add this constant factor just to have $R_f(k) \in [-1, 1]$ (note that $R_f(0) = 1$), which is easy to visualize and interpret.

To illustrate the utility of ACF in equation (3.11), lets consider an artificial profile of the form

$$g(x) = A_0 \cos\left(\frac{2\pi}{\lambda}x\right) + h_0 \tag{3.12}$$

with wavelength $\lambda \in \{50, 60\}$, amplitude $A_0 = 10$ and bias $h_0 = 100$.

On the left of Figure 3.5 we have displayed function (3.12) with $\lambda = 50$, and on the right its autocorrelation function $R_g(k)$, both in the range $\{0, 1, ..., 499\}$. Since $\lambda = 50$ is commensurable with the considered interval length, i.e. 500, it is satisfied that $R_g(k) = R_g(k + m\lambda)$ for any $k, m \in \mathbb{Z}$. In particular R_g is periodic, with period (wavelength) λ, and amplitude $R_g(0) = 1$, as it is intuitively expected and observed on the right of Figure 3.5.

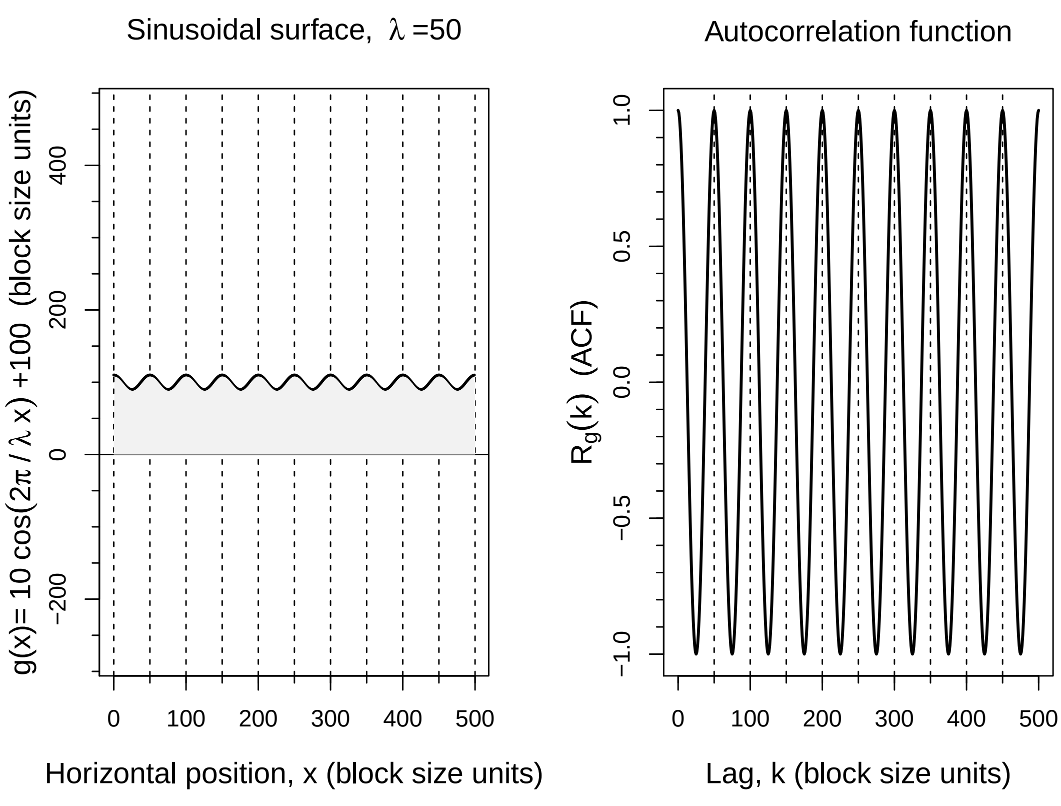

Figure 3.5: On the left, artificial sinusoidal road profile with formula $g(x) = 10\cos\left(\frac{2\pi}{\lambda}x\right) + 100$ with $\lambda = 50$, in the range $x \in [0, 499]$. On the right, it is represented the autocorrelation function for $g(x)$. The black, vertical and dashed lines indicate positions that are equispaced 50 horizontal units, i.e., in positions $\{50, 100, 150, 200, 250, 300, 350, 400, 450\}$.

The main conclusion we can extract from this case is that if we have a periodic function whose period is commensurable with the interval length (in our context, the road length), the autocorrelation function will be periodic, with the same period, and with amplitude 1. The important point is that the converse statement is also true, so if we observe an autocorrelation function of these form, this would mean that the original function is periodic and with period equal to the distance between (maxima) peaks.

However, the most probable is that given an interval length (road size), the function (road profile) we will be dealing with would probably not be purely periodic and, even if it was the case, its period would probably not be commensurable with the interval length.

We illustrate a similar case as above but by choosing a period $\lambda = 60$ which is not commensurable with 500. The results are shown in Figure 3.6.

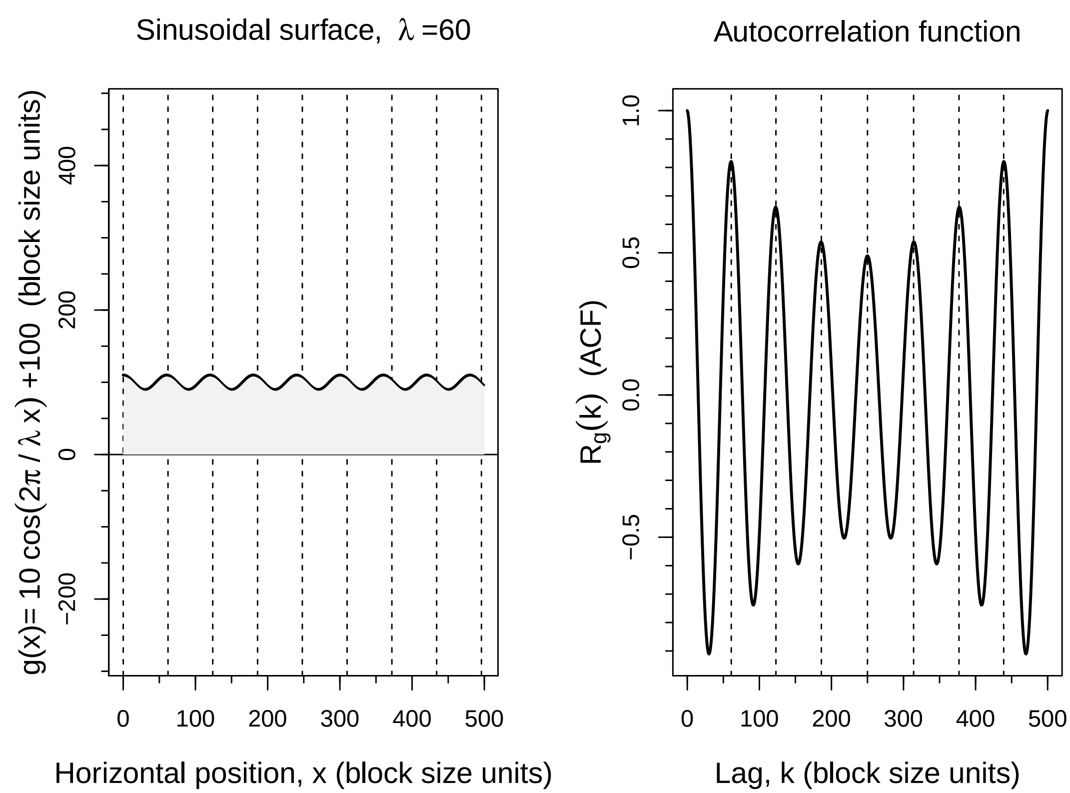

Figure 3.6: As in Figure 3.5 but with $\lambda = 60$. In these case, the vertical, black and dashed lines which correspond to the maxima of the ACF, are located at the positions $\{61, 123, 186, 250, 314, 377, 439\}$.

In contrast to the case from Figure 3.5, we now observe that the autocorrelation function has variable amplitude but is still observed to be quasi-periodic and with an approximate period $\lambda \approx 61 \pm 1$. Now the ACF has not been able to capture the exact period of the original function since, in fact, the function is not purely periodic in the strict sense, if we consider periodic boundary conditions and the definition of the ACF (3.11) we have given in the interval $[0, 499]$. However, the ACF has been able to capture the periodic nature of the original function by means of quite symmetric oscillations, and we can extract from it an estimation of the period.

Therefore, the ACF we have defined seems to be useful to analyse the periodicity of the simulated road profiles. One may have to focus on seeing if the ACF have some kind of periodicity and symmetry, and if it is the case, this well give an idea or estimation about the period of the road profile.

4 Simulation results

In this section we will show some results coming from simulations of our model. First we will study the dependence of the initial road configuration on the periodicity or quasi-periodicity of the final road configuration [5]. Then we will study the qualitative influence of some of the model parameters on the final road configurations. If it is not specified the contrary, all simulations have associated the model parameters from Table 3.1.

4.1 Dependence of washboarding on the initial road configuration

Periodic road initialization

First, lets consider a initial road with 50 irregularities equispaced a distance of $\lambda_0 = 10$ block units. In Figure 4.1 we have displayed the initial and final road profiles on the left, and the corresponding autocorrelation functions on the right. Since the initial road configuration is periodic with period λ_0; by construction, we can observe that the ACF consists of "Dirac's deltas" with amplitude 1 at positions that are multiple of λ_0, and it is zero otherwise.

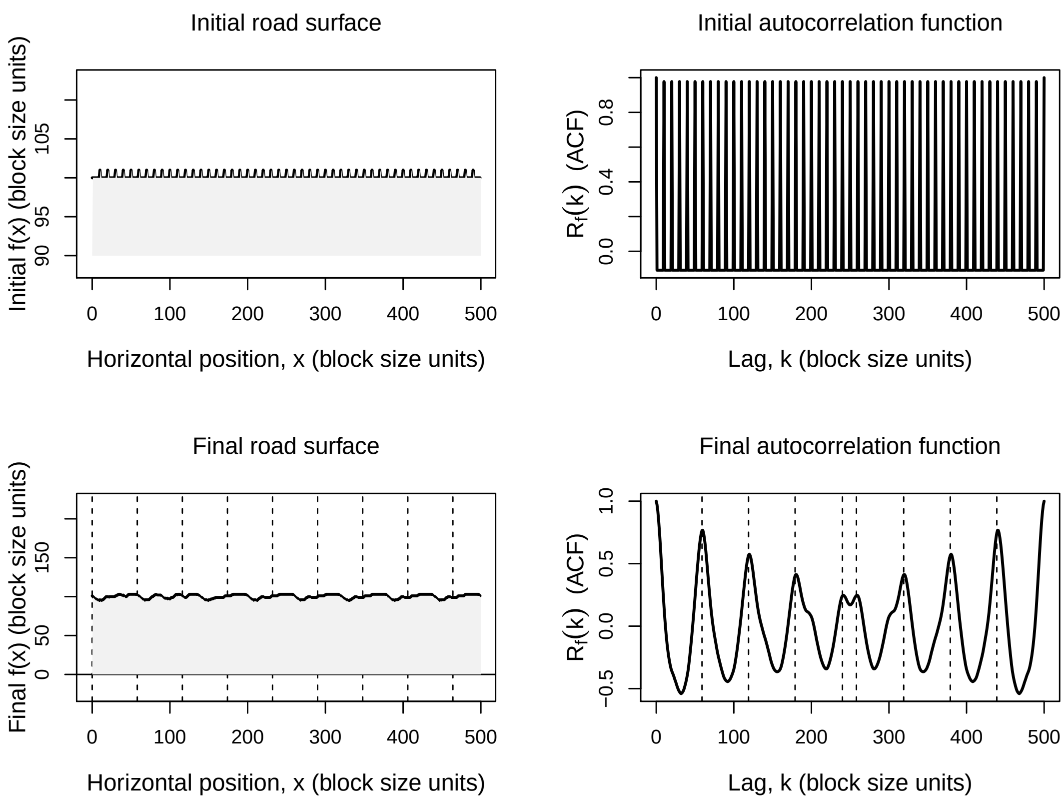

Figure 4.1: On the left, initial and final (1000 iterations) road profiles for a initial periodic road with period $\lambda_0 = 10$. On the right, the corresponding autocorrelation functions.

After 10^3 wheel passes, we can see that the resultant road profile is more or less periodic, especially

[5] The final road configuration is the one after a default number of wheel passes is performed. See Table 3.1.

in the range $\approx [150, 500]$. This periodicity is in fact reflected in the behaviour of the ACF. As can be seen from Figure 4.1, the ACF oscillates around zero and has well definite peaks of an amplitude of about 0.5 units and separated a distance $\lambda \approx 60$. This result and what we observed for the sinusoidal example (see Figure 3.6) suggest that a initial periodic road profile leads to a final more or less periodic road surface pattern with some approximated wavelength λ.

Random uniform road initialization

Next, we consider an initial road initialized by setting 50 irregularities uniformly and randomly distributed in the interval $[0, 499]$. In order to illustrate the results we consider two particular cases of random initialization which are shown in figures 4.2 and 4.3. In both cases we observe that the initial autocorrelation function is essentially zero (very small oscillations around zero), as it is expected since we are initializing with a random uniform distribution.

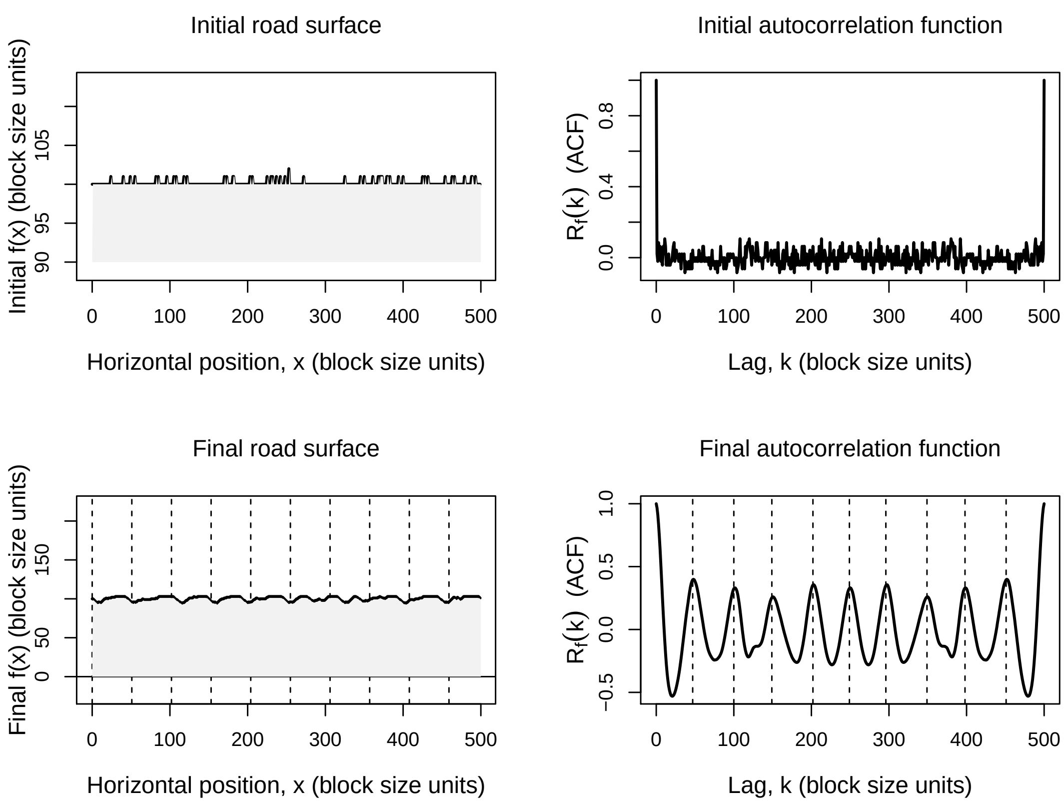

Figure 4.2: Random initialization attempt 1. On the left, initial and final (1000 iterations) road profiles for a initial road with 50 irregularities randomly and uniformly distributed among the road size. On the right, the corresponding autocorrelation functions.

In the first attempt (Figure 4.2), the final road profile looks quite periodic and the ACF also gives us evidences about this fact. Now the observed (mean) wavelength or period is about $\lambda \approx 50$. It would be estimated averaging the separations between peaks.

However, in a second attempt of random initialization (Figure 4.3), it is quite hard to distinguish some kind of periodicity on the final road profile. The ACF again presents peaks and oscillations, but now these oscillations are not very symmetric with respect to zero, and there is the presence of some higher (primary) and smaller (secondary) peaks that intercalate between them. Therefore, in this case one would say that the final road profile is more irregular or chaotic than before.

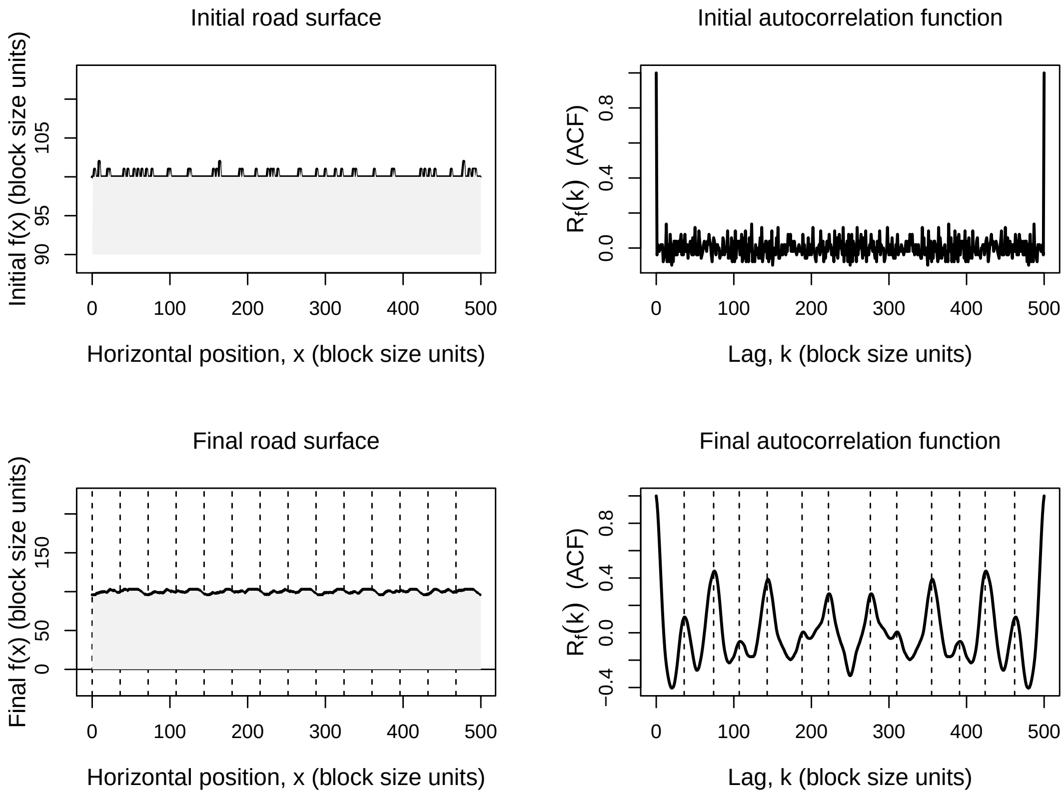

Figure 4.3: Random initialization attempt 2. On the left, initial and final (1000 iterations) road profiles for a initial road with 50 irregularities randomly and uniformly distributed among the road size. On the right, the corresponding autocorrelation functions.

An important result we have obtained is that with random initialization the final road profile tends very often to have some kind of periodic behaviour as it was observed for the periodic road initialization and the first random attempt from Figure 4.2. Moreover, our model is able to observe what was commented in section 1: *Dirt roads do not heal themselves, but instead, become progressively more corrugated [4].*

In addition, while David and Boris [3] by means of different analysis concluded that washboard patterns from their model *exhibit a non-periodic, deterministic chaotic evolution that is between regular and stochastic, noisy behaviour*; our model extension with new digging and smoothing' approaches seem to sometimes lead to regions of periodicity or quasi-periodicity, depending on the initial road configuration. However, future tasks to confirm these results would be to consider larger road sizes and analyse the patterns both locally and globally.

In the next section we are going to analyse the influence of some model parameters on the final road's profile, but without focusing on periodicity nor autocorrelation functions. Future work may include studying how the period of the final road (if any) depends on the model parameters.

4.2 Dependence of washboarding on some important model parameters

In this section we are interested in the effects of varying different important parameters like α (soil density and stiffness), β (velocity), d (wheel size or digging width), p_w (wind frequency). For these simulations we started with the same initial road with a periodic initialization seen in section 4.1. Especially we want to investigate the behaviour in terms of wave length and amplitude of the resulting road surface.

We want to stress that all plots in this section have a different scale for the x- and y-axes. On the x-axis the road is shown on full length ranging from 0 to 500. The y-axis is in contrast only ranging from roughly 90 to 105 as a road height.

Effect of digging probability distributions in terms of α

The first parameter we investigate is the digging probability parameter α. As we have seen in Figure 3.4 a higher α value leads to a heavily decreasing probability of digging if we reach lower levels of the soil.

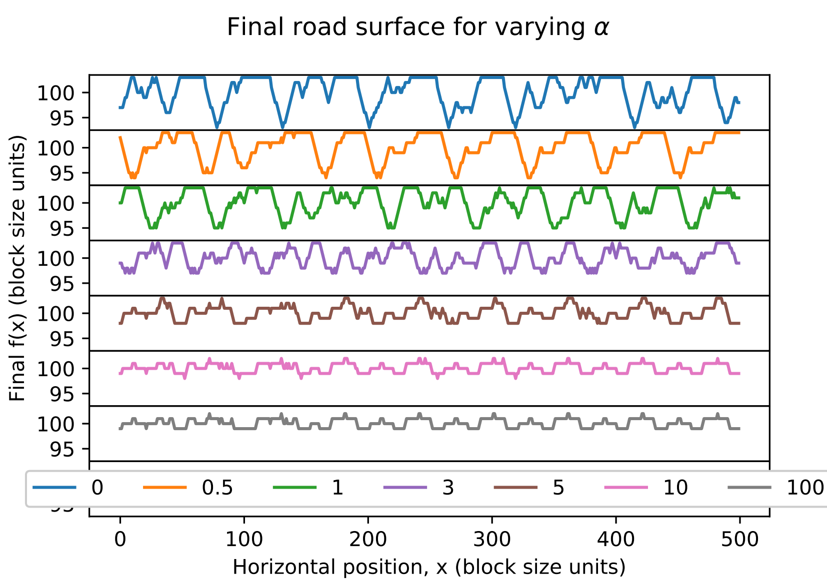

Figure 4.4: Resulting Road Surface for different α values.

In fact we can see in Figure 4.4 that we get a way smaller (negative) amplitude for high α. We can see a maximum depth of 92 (which means 8 levels below the standard height) for $\alpha = 0.1$ whereas for $\alpha = 100$ we have a maximum depth of only 99 units.

α	Max Depth
0.1	92
0.5	94
1	95
3	97
5	98
10	98
100	99

Table 4.1: Maximum Depth of Road Surfaces for different Digging Probability Distributions.

In general one can say that α is a good tool to map a specific ground density with its correlation to digging to our simulation.

Effect of the wheel's diameter (digging width) d

In this section we examine the effect of the wheel diameter **d**. From Figure 4.5 one can see that the wavelength [6] increases for increasing **d**. Furthermore we can observe that the amplitude is increasing up to a limit. This limit may be determined through the smoothing method and parameters (positive amplitude) and the digging probability distribution).

For the higher wheel sizes we observe flat areas as amplitudes. This is a result of $h_{max} = 103$ as a standard parameter which leads to a smoothing above the height $f(x) > 103$. If we would have increased the h_{max} value (and therefore reduce smoothing) we could observe bigger piles for large wheel diameters.

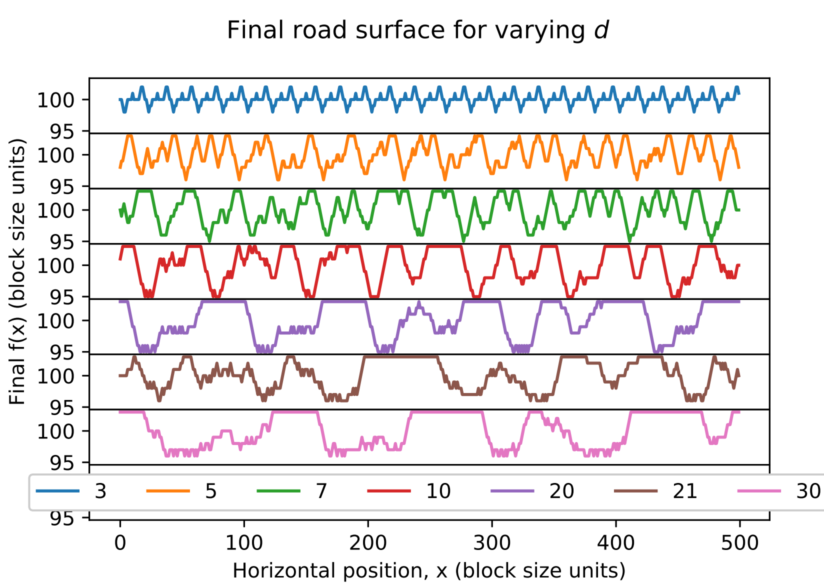

Figure 4.5: Resulting Road Surface for different Wheel Diameters.

[6]Strictly speaking we refer to "separation between peaks or bumps" or the average separation.

Lastly we want to note that the road length for large diameters seems a bit too small. In these cases we can only observe roughly 4 periods.

Effect of the velocity proportional constant β

Now we investigate the resulting road surfaces for the velocity proportional constant β. Here we notice two things.

At first the wavelength increases for greater values of β (lets say, for higher velocities). This is due to our jumping distance method which is directly proportional to the velocity proportional parameter β and the bumps' height. Therefore we can see bigger jumps and longer periods.

Secondly, the impact of the wheel with a greater velocity (proportional constant β) is bigger, which leads to deeper potholes. This effect may be an after-effect of the first observation we have done above about the jumping distance. Due to the resulting larger wavelengths, we have fewer and deeper oscillations.

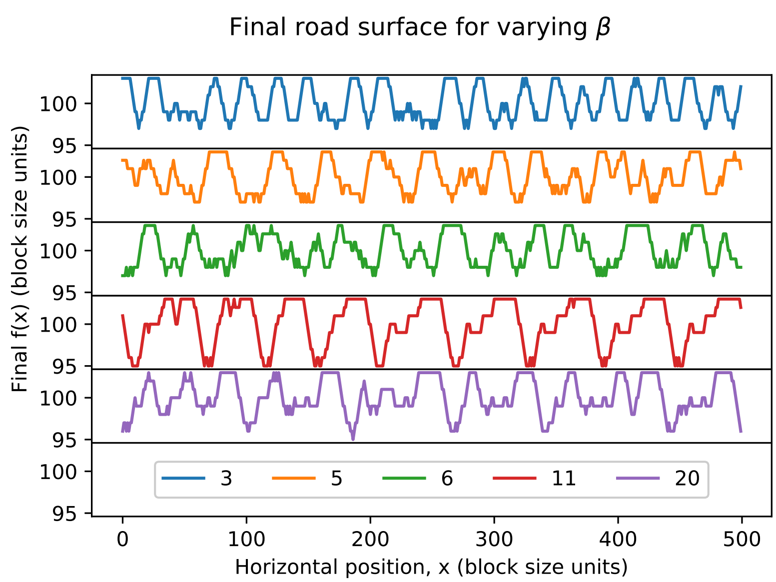

Figure 4.6: Resulting Road Surfaces for different Velocity proportional Constants.

Effect of the wind probability (wind's frequency of occurrence) p_w

Our last parameter in our investigation is the wind's frequency, i.e. how often we use the wind smoothing. From Figure 4.7 we can observe exactly three things:

1. The wave length does not change for varying p_w. This is reasonable because the wind should have no effect on the period of a road corrugation.
2. The maximum (positive) amplitude stays the same at around 103. Again this is due to the h_{max} parameters and its `max_smoothing`.
3. The maximum depth decreases for increasing wind's frequency. This behaviour is as desired because the wind carries the higher grains the minima of the road surfaces which fills the potholes.

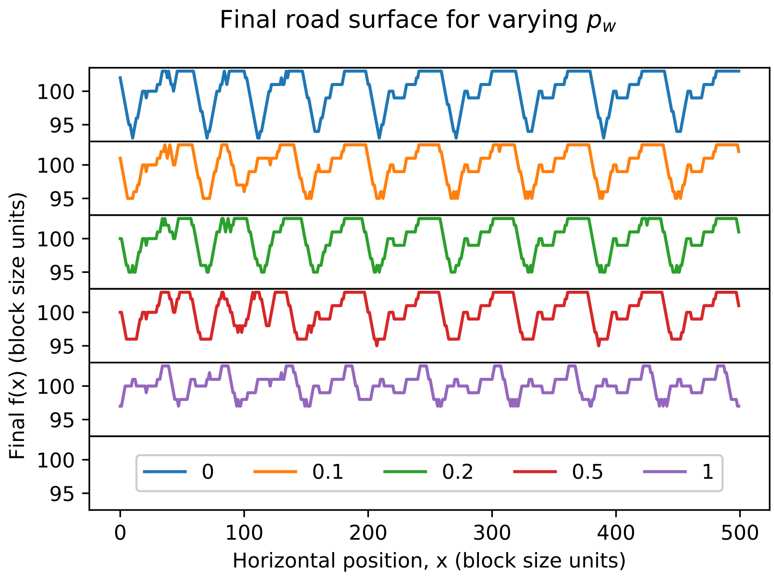

Figure 4.7: Resulting Road Surface for different Wind Occurrence Probabilities.

5 Conclusions

We mainly focused our washboard simulation investigation on two things. The differing results for roads starting from a periodic regular road surface and a random one; and the study of parameters we considered to be important and interesting like the velocity, wheel's diameter, the occurrence of the wind and the soil properties.

First we had the periodic versus the random initial road comparison. The former one seemed to led always to very periodic road surfaces. We can say that this also occurs often for random initialized roads but not in every case. Sometimes we get a more chaotic surface where it is not totally clear why and when each behaviour is to be observed.

Secondly we varied several parameters for a regular periodic road. Here we can conclude that the plots show quite good the expectations one could have for theses parameters and their properties in nature. We have filling potholes (less deep holes) for stronger (i.e. more often occurring) winds and for denser and harder soil grounds and furthermore we could show larger wavelengths for bigger wheel diameters and higher velocity proportional parameters β.

Finally, in the next section we make a discussion about the model strengths, its limitations and some future work and extensions that could be done.

6 Model strengths, limitations and future work

The model takes into account numerous observations in the published literature about washboarding, having them inserted as variables or functions into the program. Such observations are the velocity of the cars, the diameter of the tire and the flow of traffic. Furthermore, the fact that the digging effect is easier to occur near the surface than deeply, has also been taken into account in the program as a probability density distribution dependent on the height. Three observations that can be considered indirectly in the model are the pressure of the tire, the vehicle mass and the softness of the ground (see Table 6.1).

However, this model has some limitations. Based on other papers about experimentation on washboard roads, it was found out the existence of a threshold velocity for the vehicles above of which the washboarding effects started to be increasingly more relevant [4, 12]. This phenomenology is not present in our model. This could denote a lack of understanding about the actual interaction between the tire and the soil. Another limitation would be the fact that our model is quite dependent on a parameter we called h_{max}, which is a maximum height for the profile that we introduced regarding the fact that very high bumps are unstable. The point is that this parameter is forcing the behaviour of our system, we would prefer this maximum height to appear naturally due to the dynamics of our model. Also, the shape of the particles is not taken into account, as well as other specific characteristics of the soil (damping capacity, weight, coefficient of uniformity) directly, but indirectly via α in the digging model.

Table 6.1: Observations accounted and not in the model

Accounted	Non-accounted
Velocity (via β)	Threshold velocity
Diameter of tire (via $\mathbf{d}$)	Particle shape
Flow of traffic (via the number of wheel passes)	Real length scales (real units)
Pressure of the tires (indirectly, via β)	The possible impact of bi-wheel vehicles
Vehicle mass (indirectly, via β)	Angles of repose smaller than 45º
Softness of the ground (indirectly and dig model)	
Characteristics of the soil (α and smoothing model)	
Diffusion and environmental effects such as wind	
Mono wheel vehicles	

The main strength of this model is, in some way, the simplicity and intuitiveness of its "core idea": model a road as an aggregate of stacked particles. Because of this, it is quite easy to add new features to the model in order to make it more realistic. Examples of this are:

- The softness of the ground, which is modelled through the parameter α which, in turn, tunes the digging probability as a function of the height.
- The velocity of the vehicles through the parameter β, which, although it is set as constant for simplicity, it could as well be modified for each wheel pass simulating a more realistic flow of traffic.
- The diameter of the tire which is modelled by the quantity $\mathbf{d} = \mathtt{wheel}_{x_f} - \mathtt{wheel}_{x_0}$, but it has

to be thought as a digging width which could be done dependent on the tire pressure or other properties of the wheels, or quantities such as the impact velocity of the vehicle when landing onto the road after jumping.

- The pressure of the tires which is related to the parameter β. The more pressure the tires have, the more elastic will be the clash with the bump, so less energy will be dissipated in form of heat and deformations so the wheel will have more kinetic energy, increasing the jump length.
- The flow of traffic which is modelled by the number of wheel passes between smoothings, in such a way that a road with a lot of traffic would be less smoothed leading to an overall more abrupt profile.
- The mass of the vehicle is also taken into account through the β parameter. It is observed that heavier vehicles produce smaller jumps [16], which makes sense according to experience.
- Additional examples can be extracted from Table 6.1.

An immediate extension of this work would include ideas such as the following:

- Try to simulate bi-wheel vehicles instead of mono-vehicles and analyse the impact of this modification on the road patterns.
- Try to define and introduce some real scale units to the horizontal and vertical directions to compare with real experiments. So far our units are "non-dimensional squared block units".
- Try to introduce some phenomenology that models the threshold velocity by itself, without imposing it. A starting point could be to take into account the pressure that the wheel does to the ground and make the number of grains dug proportional to this pressure.
- Consider very long roads to analyse more deeply the periodic, quasi-periodic or chaotic behaviour of the final road surface patterns, both locally and globally.
- Finally, try to develop an algorithm for slope smoothing able to achieve angles of repose smaller than 45º.

References

[1] J.G. Riley. *The road corrugation phenomenon: a simulation and experimental evaluation.* Cornell Univ., 1971.

[2] Nicolas Taberlet, Stephen W. Morris, and Jim N. McElwaine. Washboard road: The dynamics of granular ripples formed by rolling wheels. *Phys. Rev. Lett.*, 99:068003, Aug 2007.

[3] David C. Mays and Boris A. Faybishenko. Washboards in unpaved highways as a complex dynamic system. *Complex.*, 5(6):51–60, July 2000.

[4] Joseph A. Both, Daniel C. Hong, and Douglas A. Kurtze. Corrugation of roads. *Physica A: Statistical Mechanics and its Applications*, 301(1):545 – 559, 2001.

[5] Antal Károlyi and János Kertész. Lattice-gas model of avalanches in a granular pile. *Phys. Rev. E*, 57:852–856, Jan 1998.

[6] Herrmann H.J. On the shape of a sandpile. *Physics of Dry Granular Media.*, 350, 1998.

[7] Rafael J. Martínez-Durá Ignacio García-Fernández, Marta Pla-Castells. A discrete model for the dynamics of sandpile surfaces. *Proceedings of the Industrial Simulation Conference*, pages 64–68, 2007.

[8] Andreas Radke. Daniel Salgado R. Spyridoula C. S., Cristian Estany B. Washboarding simulation in python. `https://github.com/schakalakka/Washboard-Road-Simulation`, 2018.

[9] Douglas Kurtze, Daniel C. Hong, and Joseph A. Both. The genesis of washboard roads. 15:3344–3346, 10 2001.

[10] Anne-Florence Bitbol, Nicolas Taberlet, Stephen W. Morris, and Jim N. McElwaine. Scaling and dynamics of washboard roads. *Phys. Rev. E*, 79:061308, Jun 2009.

[11] Valeria Barra, Boris Boutkov, JiaMing Chen, Yuxin Chen, Michael DePersio, Ensela Mema, Jimmy Moore, Juan Restrepo, Marisabel Rodriguez Rodriguez, Tural Sadigov, and Ting Wang. A smooth ride on a bumpy road - graduate student mathematical modeling camp 2014 report, 06 2014.

[12] K.B. Mather. The cause of road corrugations and the instability of surfaces under wheel action. *Civil Engineering and Public Works Review*, 57, 1962.

[13] Wikipedia contributors. Angle of repose — wikipedia, the free encyclopedia, 2018. [Online; accessed 27-January-2018].

[14] Wikipedia contributors. Autocorrelation — wikipedia, the free encyclopedia, 2018. [Online; accessed 30-January-2018].

[15] Juan Pablo Bello. Periodicity detection, Course: MPATE-GE 2623 Music Information Retrieval. New York University.

[16] R.B.L.; Carson R.M. Stoddart, J.; Smith. Transporting engineering journal. *ASCE*, page 376, 1982.

A Tables of variables and parameters

Table A.1: General program variables. All are integers.

Variable	Notation	Description	Range
`number_of_wheel_passes`	`max_iterations`	Number of total wheel rounds	$\mathbb{Z}^+$
`road_size`	r	Discrete road length or size	$\mathbb{Z}^+$
`standard_height`	h_0	Standard road height	≥ 1
`nr_of_irregular_points`	——	Number of grains to initialize the road randomly	≥ 1
`wheel_size`	$\mathbf{d}$	Wheel's diameter or digging width	$r \geq, \geq 1$
`velocity`	β	Jumping-distance's proportionality constant	≥ 1

Table A.3: Digging variables

Variable	Notation	Description	Range

`dig_method`	——	Digging procedure or method	`Backwards uniform`
			`Backwards quadratic`
			`Backwards tailed exponential`

`constant_probability`	p	Constant probability for the `backwards uniform` method	$(0, 1]$
`h0`	——	Threshold value for the normalization of dig probabilities	Default: h_0
`alpha`	α	Exponential digging distribution parameter or rate	$\alpha \in \mathbb{R}^+ \cup \{0\}$

Table A.5: Smoothing variables

Variable	Notation	Description	Range
smoothing_method	——	Smoothing procedure or strategy	strategy 1 strategy 2 strategy 3 strategy 4
h_max	$h_{\max}$	Threshold value for the max_smoothing function	$h_0 + \Delta$, $\Delta \in \mathbb{Z}^+$
increment_h_max_wind	$\Delta h_{\max,\text{wind}}$	Upper levels of soil affected by wind	$\mathbb{Z}^+$
lower_bound_increment_h_max_wind	$\Delta h_{0,\text{wind}}$	Levels above h_0 not affected by wind	$\mathbb{Z}^+$
p_wind	p_w	Probability of wind's occurrence	$[0, 1]$
slope	slope	Slope that leads to θ_r given in (3.10)	$\mathbb{Z}^+$